Check for updates

Sensitizing the phosphorescence of pyromellitic diimide through non-covalent halogen–carbonyl interactions†

Debranjan Hati, Swadhin Garain, Shagufi Naz Ansari,‡
Anju Ajayan Kongasseri and Subi J. George (iD) *

In this study, we efficiently sensitize pyromellitic diimide's triplets by cocrystallizing with heavy bromine-substituted small aromatics. The resulting halogen bonding interactions mediate an external heavy atom effect, leading to remarkable ambient phosphorescence with one of the highest quantum yields reported to date.

Arylene diimides, renowned for their versatile electron-deficient aromatic cores, have emerged as a formidable addition to the realm of functional organic and supramolecular materials.[1] Their exceptional electron-accepting capabilities and ability to exhibit fluorescence across a wide spectrum of colors have made them highly sought-after molecules in a myriad of applications, ranging from sensors to organic electronics. Despite reports on their triplet population through inter-system crossing (ISC), the ambient triplet harvesting properties of arylene diimides have been seldom explored due to the demanding prerequisites necessary for stabilizing their triplet states.[2] Recently, organic phosphors have garnered widespread attention for their plethora of applications in display technologies, sensing, anticounterfeiting, and imaging.[3] Stabilizing the triplet states in organic phosphors requires system designs with high spin–orbit coupling (SOC) to enhance the rate of ISC, often facilitated by incorporating heavy atoms into the system, while carefully considering design strategies to minimize vibrational dissipation and oxygen-induced quenching of the triplet states.[4]

In this context, arylene diimides, due to their potential to undergo facile structural modifications make them intriguing

candidates for revisiting and exploring their triplet harvesting properties. In line with this, our group has recently reported efficient phosphorescence from the smallest congener of the family, pyromellitic diimides, by introducing heavy-atom substitution at the core.[5] Another well-explored design approach involves non-covalent sensitization of the dark triplet states of organic phosphors through doping or cocrystallization with suitable components capable of introducing various non-covalent interactions to stabilize the triplet states.[6] The pioneering work by Kim *et al.* has demonstrated the potential of the aforementioned approach through a 'directed heavy atom effect', enhancing phosphorescence efficiency through simple doping.[7] Furthermore, recent efforts by the group of Würthner successfully stabilized the locally-excited triplet state (^{3}LE) of arylene diimide, specifically naphthalene diimide, using
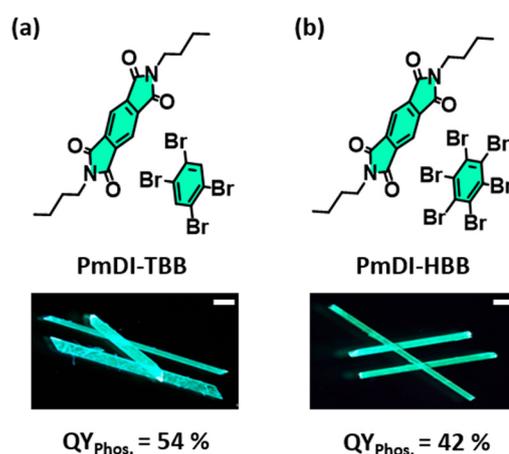
Fig. 1 Molecular structure and photographs of the cocrystals: (a) **PmDI-TBB**, and (b) **PmDI-HBB** demonstrating the halogen bond mediated cocrystallization approach to sensitize efficient room temperature phosphorescence (RTP) from pyromellitic diimide (**PmDI**) (corresponding phosphorescence quantum yields (QY$_{Phos.}$) are also mentioned). Photographs of cocrystals are taken by irradiating with 365 nm light (scale bar = 1 mm).

Supramolecular Chemistry Laboratory, New Chemistry Unit, School of Advanced Materials, Jawaharlal Nehru Centre for Advanced Scientific Research (JNCASR), Jakkur, Bangalore, 560064, India. E-mail: george@jncasr.ac.in; Fax: +91 8022760; Tel: +91 8022082964
† Electronic supplementary information (ESI) available. See DOI: https://doi.org/10.1039/d4ce00812j
‡ Present address: Department of Chemistry, School of Engineering, Presidency University Bangalore, 560064, India.

metallovalent interactions through cocrystallized heavy-platinum metal complexes.[8] Simultaneously, our group has independently achieved sensitization of the ambient triplet state emission from the charge-transfer states (^{3}CT) of pyromellitic diimide through non-covalent complexation with electron-donating molecules.[9] Moreover, Fu *et al.* recently demonstrated the sensitization of pyrene phosphorescence by cocrystallization with perylene bisimides, employing a loose cocrystal strategy.[10]

In this regard, herein we present, one of the most efficient ambient phosphorescence with the highest quantum yield to date among the reported cocrystals where phosphorescence is achieved by the external heavy atom effect. This impressive result was achieved *via* cocrystallization of **PmDI** with heavy-atom containing benzene derivatives, tetra bromo benzene (**TBB**) and hexa bromo benzene (**HBB**) (Fig. 1), by deliberately introducing halogen bonding through halogen–carbonyl interactions ('external heavy-atom effect'). Our work showcases highly efficient phosphorescence from the **PmDI** phosphor in both crystalline state (quantum yield of 54% and 42% under air for **PmDI-TBB** and **PmDI-HBB**, respectively) and in the amorphous film, marking an impressive advancement in this field.

We first investigated the spectroscopic properties of **PmDI** in THF ($[c]$ = 10^{-5} M), which shows an emission band spanning from 370 nm to 550 nm ($\lambda_{max.}$ = 410 nm, and 434 nm) with vibronic features ($\lambda_{exc.}$ = 340 nm) (Fig. 2a). The lifetime of this emission was 2.17 ns ($\lambda_{exc.}$ = 375 nm, $\lambda_{monitored}$ = 450 nm), and is attested to the locally excited fluorescence emission (^{1}LE) of **PmDI** (Fig. S1a, Table S1†). However, upon freezing at 77 K in THF, it exhibited a bright green emission (λ_{max} = 500 nm) with a lifetime of 404 ms that can be ascribed to the phosphorescence (^{3}LE) of **PmDI** (Fig. 2a and S1b, Table S1†).

Thus, in an attempt to sensitize the ^{3}LE emission from **PmDI**, we have grown 1:1 cocrystals of **PmDI** independently with **TBB** and **HBB**, which showed bright green emission under 365 nm UV irradiation (Fig. 1). Steady-state emission spectra and delayed emission spectra of these cocrystals (delay time = 1 ms) showed maxima around 500 nm in the air (Fig. S2†), which exactly overlaid with the 77 K emission spectrum of **PmDI**, hinting towards the ^{3}LE nature of emission (Fig. 2d). It is noteworthy to mention that the steady-state emission of the cocrystals (**PmDI-TBB**, **PmDI-HBB**) at room temperature was almost 36 folds enhanced than that of **PmDI** suggesting the efficiency of this triplet sensitization approach ($\lambda_{exc.}$ = 340 nm) (Fig. 2c). Further, high lifetime of the cocrystals (3.97 ms and 3.32 ms for **PmDI-TBB** and **PmDI-HBB** respectively) ($\lambda_{exc.}$ = 340 nm, $\lambda_{monitored}$ = 550 nm) (Fig. 2e, Table S2†) and increment in the lifetime and
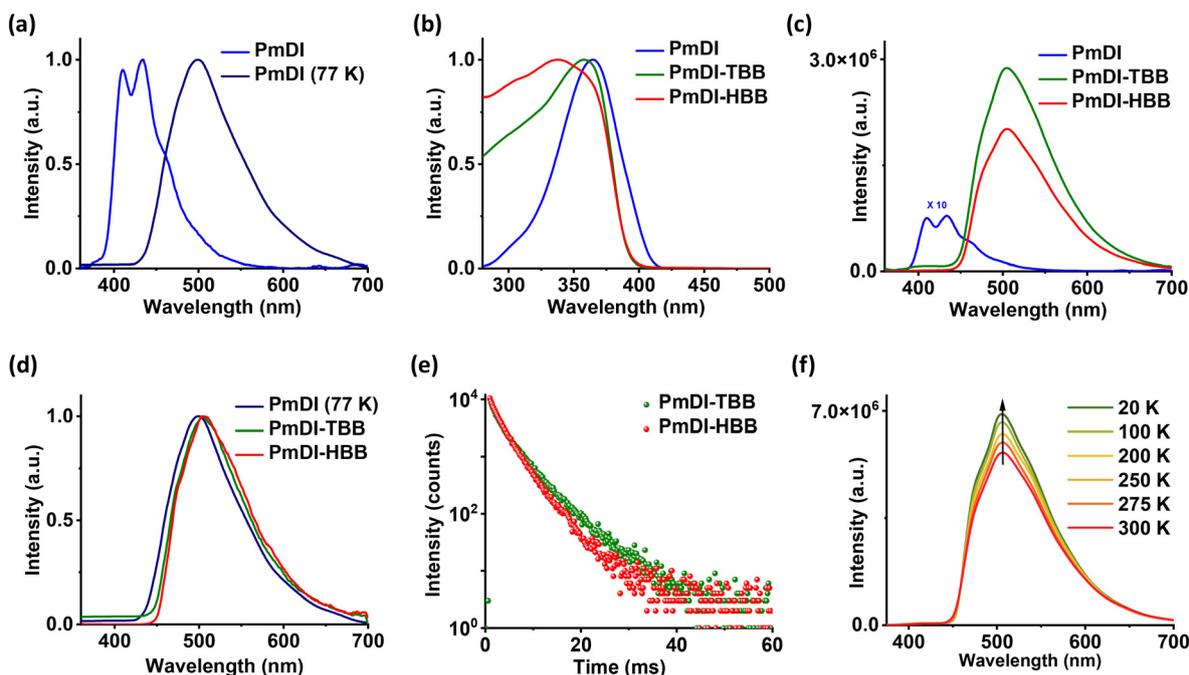
Fig. 2 Phosphorescence studies for **PmDI-TBB** and **PmDI-HBB** cocrystals: (a) normalized steady-state emission spectra of **PmDI** in $[c]$ = 10^{-5} M THF solution at room temperature (blue line) and at 77 K gated spectra (1 ms delay) (navy blue line), ($\lambda_{exc.}$ = 340 nm), showing the singlet and triplet emission, respectively. (b) Excitation spectra for individual acceptor (**PmDI**, $\lambda_{monitored}$ = 450 nm), and donor–acceptor cocrystals ($\lambda_{monitored}$ = 550 nm), which indicated the absence of charge-transfer complexation. (c) Steady-state emission spectra of **PmDI** and **PmDI-TBB**, **PmDI-HBB** cocrystals at room temperature, which shows highly emissive nature of the cocrystals compared to **PmDI** ($\lambda_{exc.}$ = 340 nm) (**PmDI** emission spectrum is multiplied by a factor of 10). (d) Normalized gated emission spectrum of acceptor in THF ($[c]$ = 10^{-5} M) at 77 K and gated emission spectra of donor–acceptor cocrystals at room temperature (1 ms delay), suggesting that source of emission is ^{3}LE state of **PmDI** ($\lambda_{exc.}$ = 340 nm). (e) Lifetime decay profile for **PmDI-TBB** and **PmDI-HBB** cocrystals ($\lambda_{exc.}$ = 340 nm, $\lambda_{monitored}$ = 550 nm). (f) Temperature-dependent steady-state emission spectra ($\lambda_{exc.}$ = 340 nm) of **PmDI-HBB** cocrystal showing the phosphorescent nature of emission.

emission intensity under vacuum confirmed the involvement of triplet state in the observed emission (Fig. S3, Table S2†). The temperature-dependent studies for both the cocrystals showed slight increase in the emission intensity and lifetime at lower temperatures, reiterating the phosphorescence (^{3}LE) nature of the emission (Fig. 2f and S4, Table S3†). Additionally, similar excitation spectra of the **PmDI** and **PmDI-TBB**/**PmDI-HBB** cocrystals ruled out the possibility of any ground-state charge-transfer (CT) interaction between them (Fig. 2b). We hypothesized that the 'external heavy atom effect' resulted in sensitization of phosphorescence emission of **PmDI** via increased SOC of the system.[8,9,11] Most interestingly, we achieved a significant phosphorescence efficiency with quantum yields (QY) of 54% and 42% in the air for **PmDI-TBB** and **PmDI-HBB** cocrystals, respectively, which increased to 79% and 44% under vacuum. Thus, it is clear that a strong external heavy-atom effect is contributing to these cocrystals, promoting substantial ISC and subsequently enhancing the efficiency of RTP in the crystalline state. This is further supported by the observed higher ISC rate (k_{ISC}) and lower non-radiative decay rate (k_{nr}) (Table S4†). The observed efficiency is the highest till now in the literature among the reported cocrystals where phosphorescence is achieved by the external heavy atom effect (Fig. S7 and S8, Table S5†). Although there are reports of doped crystals with exceptionally high quantum efficiency, they often lack a well-defined understanding of the single-crystal structure (Table S5†).[7,11d,e] We could also achieve similar phosphorescence behaviour in the solution-processable film state, which suggests that halogen bonding was intact in the amorphous films (Fig. S5†). Corresponding quantum efficiencies were found to be 12% and 13% (under air) for **PmDI-TBB** and **PmDI-HBB** respectively (Fig. S9 and S10†).

To gain deeper insight into the remarkable phosphorescence efficiencies of cocrystals via the external heavy atom effect, we performed single-crystal X-ray diffraction (scXRD) analysis of **PmDI-TBB**, and **PmDI-HBB**. We found that in the cocrystals, **TBB/HBB**, and **PmDI** formed long-range segregated stacks, and these segregated slip-stacked layers are connected via halogen bonding. For **PmDI-TBB**, one **TBB** unit interacts with two **PmDI** units via four halogen bonding interactions in the same plane. The corresponding halogen–carbonyl distances for these interactions are 3.02 Å (Fig. 3b). The Br···O distance is significantly shorter than the sum of van der Waals radii (3.35 Å).[12] In addition, halogen–π interactions are present within distances of 3.60 Å and 3.82 Å (Fig. 3c). A similar packing was observed for the **PmDI-HBB** co-crystal, where six halogen–carbonyl interactions are present with a distance of 3.01 Å, 3.05 Å, and 3.96 Å (Fig. 3e). The short intermolecular C–Br···O=C contacts (Br01···O1, 3.05 Å and Br02···O2, 3.01 Å, respectively) are shorter than the sum of the van der Waals radii (3.35 Å).[12] We envisage that halogen bonding interaction (halogen–carbonyl and halogen–π) is responsible for increase in the SOC and ISC rate of **PmDI** via the external heavy atom effect, which helped to realize bright efficient green phosphorescence emission from the ^{3}LE state.

In conclusion, highly efficient triplet emission with a phosphorescence quantum yield of 54% (under air) in the crystalline state and 13% in amorphous film from **PmDI**s is realized through the external heavy atom effect via halogen-bonding interactions. Thus, in the present work, we could expand the scope of realizing ambient phosphorescence from
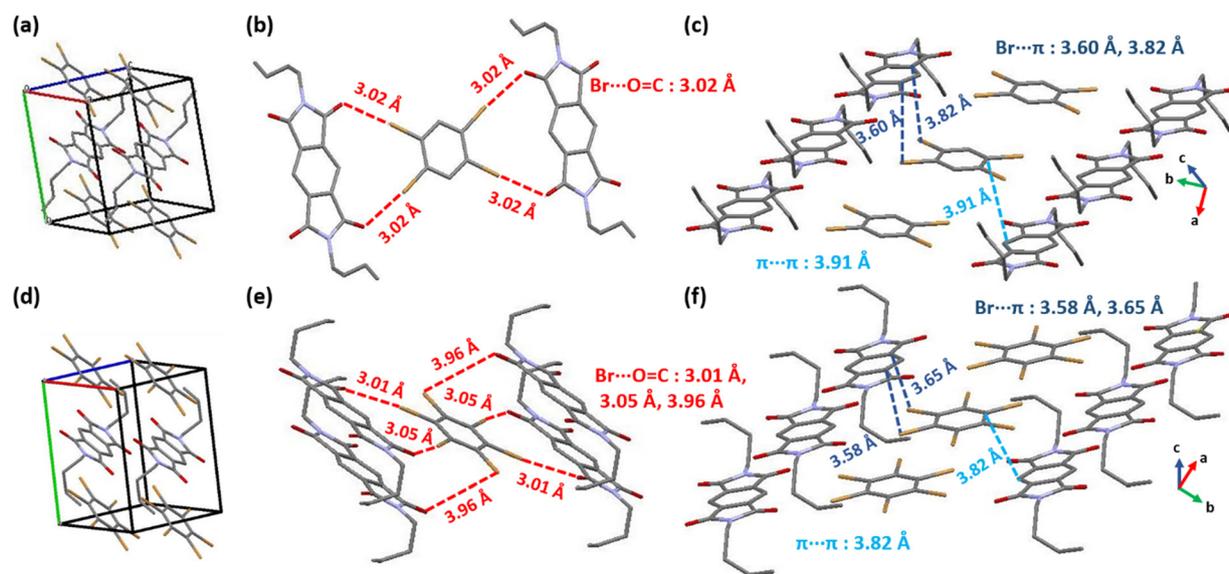
Fig. 3 Single crystal XRD data for cocrystals: **PmDI-TBB** (a–c), and **PmDI-HBB** (d–f). (a and d) Unit cell structure of **PmDI-TBB** and **PmDI-HBB** respectively. (b and e) Halogen bonding interaction and corresponding distances for (b) **PmDI-TBB**, and (e) **PmDI-HBB** (red dotted lines). In the extended structure, (c and f) Br···π interaction (navy dotted lines), and π···π interaction (sky-blue dotted lines) in between parallel planes for (c) **PmDI-TBB** and (f) **PmDI-HBB** cocrystals (red stick represents 'oxygen' atom and yellow stick represents 'bromine' atom). (CCDC: 2285499 and 2285498; refcode: CSD BOPMUS and CSD BOPMOM respectively).[13,14]

arylene diimides by this relatively easier approach, which opens up a plethora of opportunities to sensitize the triplet state of different arylene diimides in the near future. As ongoing research continues to unveil new possibilities and improvements in the triplet harvesting materials, their impact on diverse fields is expected to grow even further.

Data availability

The data supporting this article have been included as part of ESI.†

Author contributions

DH carried out all the experiments. DH and SG analyzed the data directed by SJG. SNA solved the crystal structure. DH, SG, AAK, and SJG wrote the manuscript with contributions from all authors.

Conflicts of interest

There are no conflicts to declare.

Acknowledgements

Notes and references

1 (a) F. Würthner, C. Thalacker, S. Diele and C. Tschierske, *Chem. – Eur. J.*, 2001, **7**, 2245; (b) F. Würthner, S. Ahmed, C. Thalacker and T. Debaerdemaeker, *Chem. – Eur. J.*, 2002, **8**, 4742; (c) N. Sakai, J. Mareda, E. Vauthey and S. Matile, *Chem. Commun.*, 2010, **46**, 4225; (d) S. V. Bhosale, M. A. Kobaisi, R. W. Jadhav, P. P. Morajkar, L. A. Jones and S. George, *Chem. Soc. Rev.*, 2021, **50**, 9845.

2 (a) G. N. Lewis and M. Kasha, *J. Am. Chem. Soc.*, 1944, **66**, 2100; (b) M. A. El-Sayed, *J. Chem. Phys.*, 1963, **38**, 3032.

3 (a) S. Hirata, *Adv. Opt. Mater.*, 2017, **5**, 1700116; (b) D. Sasikumar, A. T. John, J. Sunny and M. Hariharan, *Chem. Soc. Rev.*, 2020, **49**, 6122; (c) S. Xu, R. Chen, C. Zheng and W. Huang, *Adv. Mater.*, 2016, **28**, 9920; (d) B. Song, W. Shao, J. Jung, S. J. Yoon and J. Kim, *ACS Appl. Mater. Interfaces*, 2020, **12**, 6137; (e) V. C. Wakchaure, S. D. Veer, A. D. Nidhankar, Goudappagouda, R. Nayak, K. Asokan, S. Ravindranathan and S. S. Babu, *Chem. Commun.*, 2022, **58**, 1998.

4 (a) W. Zhao, Z. He and B. Z. Tang, *Nat. Rev. Mater.*, 2020, **5**, 869; (b) X. Ma, J. Wang and H. Tian, *Acc. Chem. Res.*, 2019, **52**, 738; (c) T. Zhang, X. Ma, H. Wu, L. Zhu, Y. Zhao and H. Tian, *Angew. Chem., Int. Ed.*, 2020, **59**, 11206; (d) Y. Wang, H. Gao, J. Yang, M. Fang, D. Ding, B. Tang and Z. Li, *Adv. Mater.*, 2021, **33**, 2007811; (e) A. D. Nidhankar, Goudappagouda, V. C. Wakchaure and S. S. Babu, *Chem. Sci.*, 2021, **12**, 4216; (f) H. Gao and X. Ma, *Aggregate*, 2021, **2**, e38; (g) X. Lin, J. Wang, B. Ding, X. Ma and H. Tian, *Angew. Chem., Int. Ed.*, 2021, **60**, 3459 (; *Angew. Chem.*, 2021, **133**, 3501); (h) M. S. Kwon, D. Lee, S. Seo, J. Jung and J. Kim, *Angew. Chem., Int. Ed.*, 2014, **53**, 11177 (*Angew. Chem.*, 2014, **126**, 11359); (i) D. Lee, O. Bolton, B. C. Kim, J. H. Youk, S. Takayama and J. Kim, *J. Am. Chem. Soc.*, 2013, **135**, 6325; (j) Z. Li, Y. Han, F. Nie, M. Liu, H. Zhong and F. Wang, *Angew. Chem., Int. Ed.*, 2021, **60**, 8212; (k) X. Y. Dai, M. Huo, X. Dong, Y. Y. Hu and Y. Liu, *Adv. Mater.*, 2022, **34**, 2203534; (l) S. K. Bhaumik, S. K. Panda and S. Banerjee, *Chem. Commun.*, 2023, **59**, 10396.

5 (a) S. Kuila, K. V. Rao, S. Garain, P. K. Samanta, S. Das, S. K. Pati, M. Eswaramoorthy and S. J. George, *Angew. Chem., Int. Ed.*, 2018, **57**, 17115; (b) S. Kuila, S. Garain, G. Banappanavar, B. C. Garain, D. Kabra, S. K. Pati and S. J. George, *J. Phys. Chem. B*, 2021, **125**(17), 4520; (c) S. Garain, S. Kuila, B. C. Garain, M. Kataria, A. Borah, S. K. Pati and S. J. George, *Angew. Chem., Int. Ed.*, 2021, **60**, 12323; (d) S. Garain, S. Sarkar, B. C. Garain, S. K. Pati and S. J. George, *Angew. Chem., Int. Ed.*, 2022, **61**, e2021157; (e) S. Garain, S. M. Wagalgave, A. A. Kongasseri, B. C. Garain, S. N. Ansari, G. Sardar, D. Kabra, S. K. Pati and S. J. George, *J. Am. Chem. Soc.*, 2022, **144**, 10854.

6 M. Singh, K. Liu, S. Qu, H. Ma, H. Shi, Z. An and W. Huang, *Adv. Opt. Mater.*, 2021, **9**, 2002197.

7 O. Bolton, K. Lee, J. H. Kim, K. Y. Lin and J. Kim, *Nat. Chem.*, 2011, **3**, 205.

8 M. Sun, O. Anhalt, M. B. Sárosi, M. Stolte and F. Würthner, *Adv. Mater.*, 2022, **34**, 2207331.

9 (a) S. Garain, S. N. Ansari, A. A. Kongasseri, B. C. Garain, S. K. Pati and S. J. George, *Chem. Sci.*, 2022, **13**, 10011; (b) A. A. Kongasseri, S. Garain, S. N. Ansari, B. C. Garain, S. M. Wagalgave, U. Singh, S. K. Pati and S. J. George, *Chem. Mater.*, 2023, **35**, 7781; (c) A. A. Kongasseri, S. N. Ansari, S. Garain, S. M. Wagalgave and S. J. George, *Chem. Sci.*, 2023, **14**, 12548.

10 R. Gao, Y. Cha, H. M. Ahmad, H. Fu and Z. Yu, *Adv. Opt. Mater.*, 2023, **11**, 2301112.

11 (a) A. Abe, K. Goushi, M. Mamada and C. Adachi, *Adv. Mater.*, 2023, 2211160; (b) C. Feng, S. Li, X. Xiao, Y. Lei, H. Geng, Y. Liao, Q. Liao, J. Yao, Y. Wu and H. Fu, *Adv. Opt. Mater.*, 2019, **7**, 1900767; (c) X. Pang, H. Wang, W. Wang and W. J. Jin, *Cryst. Growth Des.*, 2015, **15**, 4938; (d) L. Xiao, Y. Wu, J. Chen, Z. Yu, Y. Liu, J. Yao and H. Fu, *J. Phys. Chem. A*, 2017, **121**, 8652; (e) L. Xiao, Y. Wu, Z. Yu, Z. Xu, J. Li, Y. Liu, J. Yao and H. Fu, *Chem. – Eur. J.*, 2018, **24**, 1801.

12 A. Bondi, *J. Phys. Chem.*, 1964, **68**, 441.

13 S. N. Ansari and S. J. George, *Experimental Crystal Structure Determination*, CCDC 2285499, 2024, DOI: **10.5517/ccdc.csd. cc2gq7s7**.

14 S. N. Ansari and S. J. George, *Experimental Crystal Structure Determination*, CCDC 2285498, 2024, DOI: **10.5517/ccdc.csd. cc2gq7r6**.